Neurobiology of Disease 109 (2018) 76–87

Contents lists available at ScienceDirect

Neurobiology of Disease

journal homepage: www.elsevier.com/locate/ynbdi

A distinct microRNA expression profile is associated with α[^{11}C]-methyl-L-tryptophan (AMT) PET uptake in epileptogenic cortical tubers resected from patients with tuberous sclerosis complex

Shruti Bagla[a], Daniela Cukovic[a], Eishi Asano[a], Sandeep Sood[e], Aimee Luat[a], Harry T. Chugani[b], Diane C. Chugani[c,d], Alan A. Dombkowski[a,*]

[a] Department of Pediatrics, Wayne State University School of Medicine, Detroit, MI, USA
[b] Department of Neurology, Nemours/Alfred I. duPont Hospital for Children, Wilmington, DE, USA
[c] Research Department, Nemours/Alfred I. duPont Hospital for Children, Wilmington, DE, USA
[d] Communication Sciences and Disorders Department, College of Health Sciences, University of Delaware, Newark, DE, USA
[e] Department of Neurosurgery, Wayne State University School of Medicine, Detroit, MI, USA

ARTICLE INFO

Keywords:
Tuberous sclerosis complex
Epilepsy
Seizure
microRNA
Tryptophan
α[^{11}C]-methyl-L-tryptophan
Positron emission tomography
Gene expression

ABSTRACT

Tuberous sclerosis complex (TSC) is characterized by hamartomatous lesions in various organs and arises due to mutations in the *TSC1* or *TSC2* genes. TSC mutations lead to a range of neurological manifestations including epilepsy, cognitive impairment, autism spectrum disorders (ASD), and brain lesions that include cortical tubers. There is evidence that seizures arise at or near cortical tubers, but it is unknown why some tubers are epileptogenic while others are not. We have previously reported increased tryptophan metabolism measured with α[^{11}C]-methyl-L-tryptophan (AMT) positron emission tomography (PET) in epileptogenic tubers in approximately two-thirds of patients with tuberous sclerosis and intractable epilepsy. However, the underlying mechanisms leading to seizure onset in TSC remain poorly characterized. MicroRNAs are enriched in the brain and play important roles in neurodevelopment and brain function. Recent reports have shown aberrant microRNA expression in epilepsy and TSC. In this study, we performed microRNA expression profiling in brain specimens obtained from TSC patients undergoing epilepsy surgery for intractable epilepsy. Typically, in these resections several non-seizure onset tubers are resected together with the seizure-onset tubers because of their proximity. We directly compared seizure onset tubers, with and without increased tryptophan metabolism measured with PET, and non-onset tubers to assess the role of microRNAs in epileptogenesis associated with these lesions. Whether a particular tuber was epileptogenic or non-epileptogenic was determined with intracranial electrocorticography, and tryptophan metabolism was measured with AMT PET. We identified a set of five microRNAs (miR-142-3p, 142-5p, 223-3p, 200b-3p and 32-5p) that collectively distinguish among the three primary groups of tubers: non-onset/AMT-cold (NC), onset/AMT-cold (OC), and onset/AMT-hot (OH). These microRNAs were significantly upregulated in OH tubers compared to the other two groups, and microRNA expression was most significantly associated with AMT-PET uptake. The microRNAs target a group of genes enriched for synaptic signaling and epilepsy risk, including *SLC12A5*, *SYT1*, *GRIN2A*, *GRIN2B*, *KCNB1*, *SCN2A*, *TSC1*, *and MEF2C*. We confirmed the interaction between miR-32-5p and *SLC12A5* using a luciferase reporter assay. Our findings provide a new avenue for subsequent mechanistic studies of tuber epileptogenesis in TSC.

1. Introduction

Tuberous sclerosis complex (TSC) is an autosomal dominant genetic disorder that occurs due to mutations in either *TSC1* or *TSC2* genes, leading to altered expression or dysfunction of hamartin or tuberin proteins, respectively. These two proteins form a complex that modulates the activity of mechanistic target of rapamycin (mTOR). TSC is characterized by hamartomatous lesions in multiple organs, including brain, skin, kidney, and lung. Brain lesions include cortical tubers, subependymal nodules, and subependymal giant cell astrocytomas (SEGAs). Approximately 60% of TSC patients suffer from medically intractable seizures that are resistant to pharmacological treatment

* Corresponding author at: Division of Clinical Pharmacology and Toxicology, Department of Pediatrics, Room 3L22, Children's Hospital of Michigan, 3901 Beaubien Blvd, Detroit, MI 48201, USA.
E-mail address: domski@wayne.edu (A.A. Dombkowski).

http://dx.doi.org/10.1016/j.nbd.2017.10.004
Received 2 March 2017; Received in revised form 9 September 2017; Accepted 6 October 2017
Available online 07 October 2017

Table 1
Demographics and clinical categories for TSC patients and tissue samples. All tubers were visible on MRI and characterized for seizure onset status (onset or non-onset) by ECoG. AMT-PET uptake was classified as 'hot' or 'cold.' Samples used in microRNA arrays and qPCR validations are indicated by 'Mi' and 'P' respectively. A representative subset of these samples was used for gene expression microarrays, indicated by 'Ge.'

Sample	Patient ID	Age at surgery	Gender	Hemisphere	Mutation	Tuber	Sz Onset	AMT	Group	Location	Analyses
1	82506	4 y 9 m	F	Right	TSC2	Tuber	Onset	Hot	OH	Frontal	Mi, P
2	83002	3 y	F	Left	TSC2*	Tuber	Non onset	Cold	NC	Temporal	Mi, GE, P
3						Tuber	Onset	Hot	OH	Parietal	Mi, GE, P
4						Tuber	Onset	Cold	OC	Temporal	Mi, GE, P
5	111400	6 y	M	Right	TSC1*	Tuber	Non onset	Cold	NC	Temporal	Mi, P
6	81603	8 y	M	Left	TSC2	Tuber	Non onset	Cold	NC	Temporal	Mi, P
7						Tuber	Onset	Hot	OH	Frontal	Mi, P
8						Tuber	Non onset	Cold	NC	Temporal	Mi, P
9	92804	7.5 y	F	Left	unknown	Tuber	Onset	Cold	OC	Frontal	Mi, P
10						Tuber	Non onset	Cold	NC	Frontal	Mi, P
11	F0508	9 m	M	Left	TSC2	Tuber	Onset	Hot	OH	Central frontal	Mi, GE, P
12						Tuber	Onset	Hot	OH	Occipital	Mi, P
13						Tuber	Onset	Hot	OH	Occipital	Mi, P
14						Tuber	Onset	Hot	OH	Central frontal	Mi, P
15	G2710CC	2 y	M	Right	TSC2	Tuber	Non onset	Cold	NC	Temporal	Mi, P
16						Tuber	Onset	Cold	OC	Occipital	Mi, P
17	I1710AC	5 y	M	Left	TSC2	Tuber	Onset	Cold	OC	Frontal	Mi, GE, P
18						Tuber	Non onset	Cold	NC	Frontal	Mi, GE, P
19	I1914MC	13 m	F	Left	TSC2	Tuber	Onset	Hot	OH	Occipital	Mi, P
20	J1513AB	11 y	F	Left	TSC2	Tuber	Onset	Cold	OC	Frontal parietal	Mi, P
21	L1412RK	2 y	M	Right	TSC2*	Tuber	Onset	Hot	OH	Frontal	Mi, P
22						Tuber	Non onset	Cold	NC	Frontal	Mi, P

(Chu-Shore et al., 2010). In these cases surgical intervention to resect epileptogenic tubers is often successful in reducing seizure frequency (Weiner et al., 2006; Jansen et al., 2007; Ibrahim et al., 2015; Arya et al., 2015).

Positron emission tomography (PET) serves an important role in understanding brain development and neurodevelopmental disorders (Kumar and Chugani, 2008). The PET tracer α[^{11}C]-methyl-L-tryptophan (AMT) measures tryptophan metabolism via serotonin and/or kynurenine pathways (Kumar et al., 2011). Increased AMT uptake has been demonstrated to identify epileptogenic tubers in approximately two-thirds of patients with tuberous sclerosis and intractable epilepsy (Kumar et al., 2011; Kagawa et al., 2005; Fedi et al., 2003; Asano et al., 2000). AMT PET detected epileptogenic tubers with 74% sensitivity, 100% specificity, and 82% accuracy, as defined by seizure-free surgical outcomes (Kagawa et al., 2005). Therefore, AMT serves as an important biomarker of epileptogenic foci in TSC patients (Kumar et al., 2011; Chugani, 2011). Inflammatory response signaling is believed to be involved in AMT PET uptake in seizure onset lesions (Juhasz et al., 2013). Increased AMT uptake reflects increased tryptophan metabolism due to activation of the kynurenine pathway (Zitron et al., 2013). Indoleamine 2,3-dioxygenase (*IDO1*) is the key rate-limiting enzyme in the kynurenine pathway, and elevated *IDO1* expression is correlated with AMT uptake in epileptogenic tubers (Chugani, 2011). However, ~25% of seizure onset tubers do not have increased uptake of AMT, suggesting multiple mechanisms involved in tuber seizure propensity.

MicroRNAs (miRNAs) are a class of small non-coding RNAs that are important regulators of gene expression at the post-transcriptional level. In their mature form of 18–22 nucleotides, miRNAs anneal to complimentary sites in the 3′-untranslated region of target transcripts, causing either degradation of the transcript or inhibition of protein synthesis. A single miRNA can target multiple transcripts, and a single gene can be targeted by multiple miRNAs (Ebert and Sharp, 2012). MiRNAs have been implicated in numerous biological and pathological processes, including several neurodegenerative disorders (Szafranski et al., 2015; Nelson et al., 2008; Meza-Sosa et al., 2012). Among human organs, the brain is most enriched with microRNAs, likely owing to its functional complexity (Kosik, 2006). Several studies have demonstrated the role of miRNAs in epilepsy (Risbud and Porter, 2013; Liu et al., 2010; Jimenez-Mateos et al., 2011; Aronica et al., 2010; Schouten et al., 2015; Roncon et al., 2015). We recently reported aberrant miRNA expression in epileptogenic TSC tubers, compared to patient matched non-tuber tissue (Dombkowski et al., 2016). To further discern microRNA activity that is specifically associated with seizure onset in tubers, with and without increased tryptophan metabolism measured by AMT PET, as opposed to microRNAs that may be involved in tuber formation, we performed the present study to directly compare microRNA expression profiles in epileptogenic and non-epileptogenic tubers. This approach allowed us to focus on microRNAs that are likely involved in seizure onset. Additionally, we performed gene expression analysis in a subset of samples to identify epilepsy-risk genes targeted by the differentially expressed miRNAs.

2. Material and methods

2.1. TSC patients and tissue classification

All human brain tissue used in this study was removed as a part of planned surgery for refractory epilepsy in patients diagnosed with TSC. To obtain brain specimens following surgery for research purposes, informed consent was obtained from parents or legal guardians for all minors undergoing treatment. Collection and analysis of specimens was carried out in accordance with an approved Institutional Review Board protocol.

The 13 patients in this study underwent either a one-stage or two-stage surgery with subdural electrodes to identify regions responsible for generating habitual seizures. Anti-epileptic medications were withheld or reduced until a sufficient number of habitual seizures (typically not less than three events) were captured. Seizure onset zones were marked, with visual assessment, by a board-certified clinical neurophysiologist (E. Asano). Seizure onset was defined as a sustained rhythmic change on electrocorticography (ECoG) clearly distinguished from the background activity and accompanied by the habitual semiology not merely explained by state changes (Asano et al., 2009). Additional preoperative diagnostic assessment for identification of TSC lesions included, but was not limited to, MRI, FDG PET, and AMT PET scans (AMT PET was obtained under a clinical research protocol). Initial scalp EEG analysis was performed blinded to PET analysis. Together, along with other imaging (MRI) and clinical data, these results were used to lateralize the seizure onset region and guide the ECoG grid placement. The ECoG grid typically covered a region larger than the

area having elevated AMT-PET uptake. Final determination of specific seizure onset zones was made entirely from ECoG data. Sample characteristics are presented in Table 1. A small portion of fresh tissue collected from surgery was stored in RNAlater (Qiagen) to preserve RNA prior to extraction, while remaining tissue was frozen and stored at − 80 °C for future experiments.

2.2. RNA isolation

The "miRNeasy Mini Kit" (Qiagen, Valencia, CA) was used to isolate total RNA, including miRNA, from frozen brain tuber samples. Disruption and homogenization of 25–35 mg of tissue in 700 µl Qiazol was performed using a TissueLyser LT (Qiagen) according to the vendor's protocol. All other RNA isolation steps were done according to the protocol. The RNA integrity of each sample was tested using an Agilent 2100 Bioanalyzer and RNA 6000 Nano Assay Kit (Agilent Technologies, Palo Alto, CA).

2.3. microRNA expression microarrays

The miRNA Labeling Kit from Agilent Technologies was used to label RNA for each sample. The reaction included 100 ng of total RNA and Agilent control miRNA spike-ins. Labeled samples were then hybridized onto SurePrint G3 Human v21 8X60K miRNA arrays (Agilent Technologies, Palo Alto, CA). All steps were performed as previously described in Dombkowski et al. (Dombkowski et al., 2016). Microarray slides were scanned for fluorescent intensities using an Agilent dual laser scanner. Tiff images were analyzed with Agilent's feature extraction software (version 10.7.1.1).

2.4. Gene expression microarrays

Global gene expression profiling was performed on a subset of samples using gene expression microarrays. Total RNA, isolated as described above, was fluorescently labeled and processed as described in (Edwards et al., 2016).

2.5. Data analysis

Microarray data were imported into GeneSpring v14.5 for data analysis. The data were quantile normalized to ensure similar distributions of signal intensities on each microarray. Filtering was used to select microRNAs flagged as "detected" in ≥ 65% of samples for at least one or more sample categories (NC, OC, OH). Statistical analysis was performed to compare each pair of categories using a moderated *t*-test. A multiple test correction of *P* values was performed using the Westfall and Young permutation method to control the family-wise error rate.

2.6. DNA isolation and AmpliSeq analysis of TSC variants

TSC mutations were identified through either clinical genotyping (Athena Diagnostics) or in-house sequencing. In-house sequencing was performed on a subset of samples using genomic DNA isolated from 25 mg of frozen brain tissue. TissueLyser LT and DNeasy Blood & Tissue Kit (Qiagen) were used following the vendor's protocol. The concentration of DNA in all samples was determined using Qubit 2.0 fluorometer and Qubit dsDNA HS Assay Kit (Thermofisher/Life Technologies). The Ion AmpliSeq primer design tool was used to create 2 custom multiplex primer pools for human *TSC1* and *TSC2* genes. Two Ion AmpliSeq libraries were prepared per sample using reagents from Ion AmpliSeq Library Kit 2.0 and our 2 custom multiplex primer pools following the vendor's protocol. Ion PGM Hi-Q Sequencing Kit and Ion 316 v2 Chips were used for sequencing barcoded Ion AmpliSeq libraries (8 libraries per chip). Libraries were sequenced on an Ion Torrent PGM and variant analysis was performed using the Torrent VariantCaller v5.

2.7. miRNA target prediction

We used the Combinatorial miRNA Target Prediction Tool, CoMIR (http://www.benoslab.pitt.edu/comir/) to identify genes predicted as targets by our miRNAs of interest. To identify high confidence targets having sites for more than one of our microRNAs of interest we calculated a summed score for each target gene derived from the CoMIR probability score of the individual microRNAs of interest (miRNAs-142-3p, 142-5p, 223-3p, 32-5p and 200b-3p). We selected genes having a total score ≥ 3 (maximum of 5) for subsequent anti-correlation analysis. Spearman's rho was used to measure the correlation between microRNA expression (from qPCR) and microarray gene expression for predicted target genes. Correlation coefficients were calculated for all microRNA/gene interactions where the CoMir prediction score ≥ 0.8, and a gene specific P-value was derived based on the strongest anti-correlation for that gene.

2.8. Reverse transcription (RT) and quantitative real-time PCR

2.8.1. miRNA expression validation

For each sample 200 ng of total RNA was reverse transcribed into cDNA using the Universal cDNA Synthesis kit (Exiqon Inc., Woburn, MA) in a 40 µl reaction. Samples were incubated at 42 °C for 60 min, followed by heat-inactivation at 95 °C for 5 min. cDNA was immediately used for qPCR or stored at − 20 °C.

For quantitative Real-time PCR (qPCR), cDNA from reverse transcription was diluted three-fold in nuclease-free water (80 µl NFW in 40ul cDNA reaction mix). 4 µl of the diluted cDNA was used for each qPCR reaction using the RT-PCR SYBR Green Master Mix (Exiqon Inc., Woburn, MA). ROX (Affymetrix Inc., Santa Clara, CA) was used as a passive reference dye. LNA primers for miRs-223-3p, 142-3p, 142-5p, 200b-3p, 32-5p and 103a-3p were purchased from Exiqon. Each sample was run in duplicate. Standard SYBR Green PCR reaction was run with melt curve analysis and automatic baseline and threshold settings on an ABI Real-time 7500 PCR machine. To identify a robust endogenous control having stable expression among the sample set, we used the microRNA array data to calculate the coefficient of variance (CV) across all samples for each microRNA. We selected miR-103a-3p as our endogenous control because it had a low CV (5.9%) and a moderately high expression level. The delta Ct (dCt) method was used with miR-103a-3p as the endogenous control. For each microRNA the mean dCt value (log2) of all samples was calculated and then subtracted from each tuber dCt to obtain mean-centered dCt values. The negative of the mean-centered dCt was used as the relative expression value in subsequent analyses (Supplementary Table 1). For OH/NC matched-pair analysis the fold change was calculated from the difference in relative expression of patient-matched OH and NC tissue. Two NC samples were available for subject 81603, so the mean NC value was used in the fold change calculation for this subject. Statistical analysis of RT-PCR data was performed in JMP12.

2.8.2. Gene expression validation

For selected samples, as indicated in Table 1, 500 ng of total RNA was reverse transcribed using Taqman Reverse Transcription Kit (Applied Biosystems) in a 30 µl reaction mix. Random hexamers were used for cDNA synthesis, and the reaction was carried out at 37 °C for 1 h, followed by heat-inactivation at 95 °C for 5 min. cDNA was immediately used for qPCR or stored at − 20 °C for future use. Taqman gene expression assays were purchased from Applied Biosystems for *GRIN2A* (Hs00168219_m1), *GRIN2B* (Hs00168230_m1), *KCNB1* (Hs00270657_m1), *SCN2A* (Hs01109871_m1), *MEF2C* (Hs00231149_m1), *SYT1* (Hs00194572_m1), *SLC12A5* (Hs00221168_m1), *TSC1* (Hs00184423_m1), and *GAPDH* (Hs02758991_g1). For each sample, 20ul reaction was prepared using 2x Taqman Advanced Fast Master Mix, 1 µl primer-probe mix and 9 µl diluted cDNA in duplicates. The standard Taqman reaction was run on

an ABI 7500 or ABI QS3 instrument. The delta Ct method was used with *GAPDH* as an endogenous control.

2.8.3. Luciferase reporter assay

A microRNA expression vector for miR-32 (HmiR0147-MR04) was purchased from Genecopoeia along with the Dual Luciferase vector expressing both Renilla and Firefly genes. The luciferase reporter gene included the 3′-UTR sequence of *SLC12A5* (HmiT061441-MT06). COS7 cells were plated at a density of 40,000 cells per well in a 96-well opaque bottom plate overnight. Cells were then transfected using Lipofectamine 3000 (Promega) using the manufacturer's protocol with the dual luciferase vector and the respective miR-expression vector, in a ratio of 1:3, 1:4 and 1:5. Each well received a total of 200 ng of DNA and each sample was run in triplicate. A scrambled miRNA expression vector (CmiR0001-MR04) was used as a negative control. The Dual-Glo Luciferase assay was run according to the manufacturer's protocol (Promega). Total luminescence was measured for Firefly and Renilla using SoftMax Pro software and Flex Station 3 instrument.

We optimized the SLC12A5:miR-32 transfection ratio for stable luciferase expression and selected 1:4. For each firefly and renilla measurement, the respective average background was subtracted. For each well, firefly intensity was divided by the renilla value. Average firefly/renilla was calculated for each sample, and the ratio of miR expression vector and scrambled control was calculated. Standard error of means was used in the graphical representation.

3. Results

3.1. Identification and validation of differentially expressed (DE) microRNAs in seizure onset/AMT-hot tubers

For each patient MRI, ECoG, and AMT PET data were analyzed to characterize each tissue sample used in the study. Samples were classified by: 1) presence or absence of tubers/lesions; 2) seizure onset activity, and 3) AMT uptake, designated as hot or cold, as we previously described (Kagawa et al., 2005). Using microarrays we measured microRNA expression in 22 samples (Table 1) representing three categories of tissue: 1) seizure onset/AMT hot tubers (OH, n = 9); 2) seizure onset/AMT cold tubers (OC, n = 5); and 3) non-onset/AMT cold tubers (NC, n = 8).

We first filtered the microRNA array expression data to identify microRNAs flagged as “detected” in at least one of the three categories, resulting in selection of 788 miRs for subsequent statistical analysis. Hierarchical clustering revealed that the NC and OC tubers were most similar based on expression of the 788 microRNAs (data not shown). Statistical analysis of each pair of categories further supported this observation. We used a stringent family-wise error rate cutoff of $P \leq 0.05$ and a minimum 2-fold change to select differentially expressed microRNAs. The family-wise error rate means that the probability of having one or more false positives among the complete set of significant microRNAs is only 0.05. With these criteria we found five significant microRNAs when comparing OH to OC, one microRNA from the OH to NC comparison, and no statistically significant microRNAs in the OC to NC comparison. The statistically significant microRNAs are listed in Table 2. The results suggested that the greatest effect on microRNA expression among the groups was associated with AMT PET uptake.

Using quantitative real-time PCR (qPCR), we confirmed expression patterns for five miRNAs: miR-142-3p, miR-142-5p, miR-223-3p, miR-200b-3p, and miR-32-5p. Each of these microRNAs was confirmed to be to be significantly upregulated in onset/AMT-hot tubers, consistent with the microarray results (Fig. 1). While not statistically significant, a pattern of intermediate expression in the onset/AMT-cold tubers is also evident for several of the microRNAs, with median OC expression levels between NC and OH values. The microRNA qPCR data are available in Supplementary Table 1.

Table 2
Statistically significant microRNAs upregulated in seizure onset/AMT-hot tubers per microarray data. Six microRNAs were differentially regulated in onset/AMT-hot tubers (OH) as compared to non-onset/AMT-cold (NC) or onset/AMT-cold tubers (OC) per microRNA expression arrays. Statistical cutoffs for differential expression were: 1) corrected family-wise error rate $P \leq 0.05$, and 2) fold-change > 2.0.

	Systemic name	Corrected p-value	Fold-change	Mirbase accession number
OH vs. OC	mir-142-5p	0.00E00	+ 16.0	MIMAT0000433
	mir-32-5p	3.03E-02	+ 12.2	MIMAT0000090
	mir-18b-5p	2.02E-02	+ 4.1	MIMAT0001412
	mir-142-3p	2.02E-02	+ 3.3	MIMAT0000434
	mir-223-3p	2.02E-02	+ 2.0	MIMAT0000280
OH vs. NC	mir-200b-3p	3.03E-02	+ 6.1	MIMAT0000318

To explore inter-subject variation and the effect of unmatched samples in our dataset, we analyzed expression changes between patient-matched tissues. Our sample set includes three matched pairs of the OH/NC comparison (subjects 83002, 81603, L1412). We calculated the change in microRNA expression between matched OH and NC samples for each of these subjects. The OH/NC fold change (log2) of microRNA expression for each patient-matched comparison is shown in Fig. 2. The results reveal comparable trends of microRNA induction for each patient. While some variability in the magnitude of induction between subjects is apparent, that is anticipated given the many factors that contribute to variations in gene expression measurements of surgical samples, such as sample handling at time of collection, age of tissue archive, heterogeneity of tuber tissues, inter-subject variability, etc. The trend of expression changes observed in the matched pairs is consistent with those measured in the overall sample set, including unmatched samples where only one type of tuber was available from a subject.

3.2. miR-142-3p and miR-223-3p are strongly correlated and highly expressed in seizure onset/AMT-hot tubers

Fig. 3 shows qPCR expression values of miR-142-3p and miR-223-3p for each sample. All seizure onset/AMT-hot tubers had high levels of the two microRNAs. Additionally, a striking correlation is evident in the expression of miR-142-3p and miR-223-3p ($R^2 = 0.93$). This suggests common regulation and/or a common origin of the two microRNAs. These microRNAs have been reported to be expressed in a range of cell types, including macrophages, neurons, astrocytes, and microglia (Xu et al., 2014; Chaudhuri et al., 2013; Wang et al., 2015). Since microglia have been associated with epileptogenecity of TSC tubers (Boer et al., 2008), we quantitatively measured the level of microglial markers in our samples. HLA-DRs are established markers of microglia (Boer et al., 2008; Boer et al., 2006); therefore, we used qPCR to measure expression of *HLA-DRA* and *HLA-DRB4* in each tuber. We found only a weak correlation between *HLA-DRA* and the two microRNAs, with $R^2 = 0.28$ and 0.31 for miR-223-3p and 142-3p, respectively. *HLA-DRB4* was undetected in our patient samples.

3.3. The three tuber categories can be accurately predicted by their microRNA expression profile

We sought to determine if the collective set of five microRNAs have a unique expression pattern that distinguishes the three categories of tubers. To fully explore this question we applied linear discriminant analysis (LDA) to the qPCR data of the five microRNAs. LDA is a computational method that uses linear combinations of a set of input variables (e.g. microRNAs) to predict categorical membership (e.g. onset, non-onset, AMT) (Pereira et al., 2009). It is a dimensional reduction technique that can reduce the dimensional representation of many variables (numerous microRNAs) into fewer dimensions (e.g. two

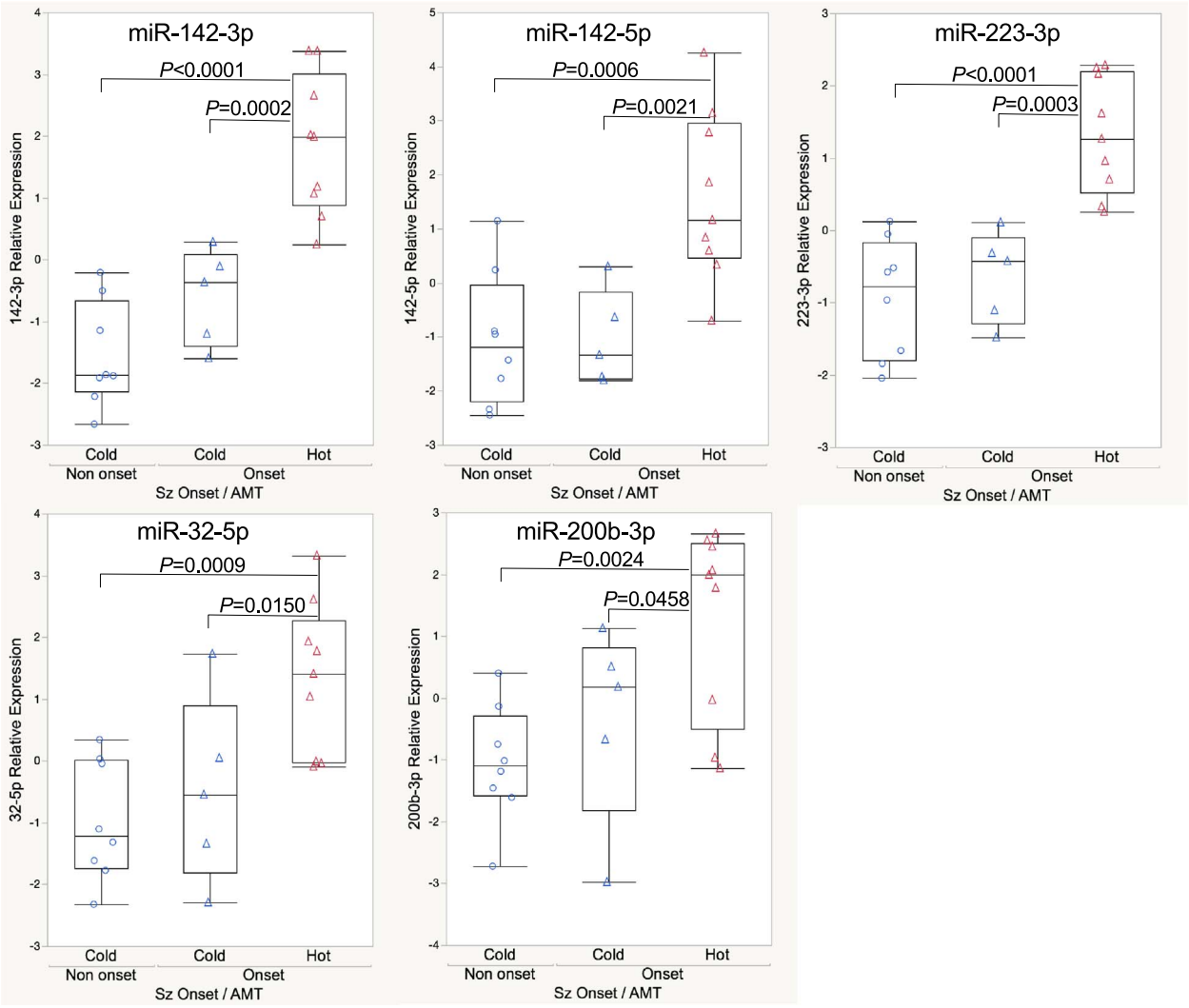

Fig. 1. qPCR validation of differentially expressed microRNAs. Five of the differentially expressed microRNAs (Table 2) were validated using qPCR. Blue circles indicate non-onset/AMT-cold tubers, blue triangles indicate onset/AMT-cold tubers, and red triangles indicate onset/AMT-hot tubers. Consistent with our microRNA array data, there was significant upregulation of these miRNAs in OH samples as compared to NC or OC. Relative expression is in log2 units. P values are shown for statistically significant comparisons.

or three) to facilitate interpretation. This method selects linear combinations of variables to maximize the separation of sample categories. We used LDA to determine if the expression profile of the aggregate set of five microRNAs is predictive of the three primary seizure onset categories (OH, OC, and NC). Using LDA derived linear combinations of expression values for the five microRNAs, we plotted the position of each of the surgical samples onto a three-dimensional representation of the microRNA expression (Fig. 4). The results reveal a clear separation of sample categories based on the expression profile of the five microRNAs. Notably, expression levels of the five microRNAs are predictive of the three tuber categories. Using microRNA expression the category for each sample was correctly predicted in 95% of cases. The onset/AMT-cold tubers have an intermediate expression profile in between the OH and NC tubers, suggesting a relationship between microRNA expression and the epileptogenic progression from non-onset/AMT-cold to onset/AMT-cold to onset/AMT-hot.

3.4. Genes involved in synaptic processes and epilepsy risk are targeted by the differentially expressed microRNAs

To identify genes targeted by the five microRNAs we integrated computational predictions with gene expression profiling to arrive at a high confidence set of targets. Each miRNA can target multiple genes and therefore regulate several pathways and cellular processes (Ebert and Sharp, 2012). Additionally, each gene may be targeted by multiple microRNAs. Therefore, it is important to consider the combinatorial effect of microRNAs on gene regulation (Dombkowski et al., 2011). To identify predicted combinatorial target genes of the DE miRNAs we used the online program CoMir (http://www.benoslab.pitt.edu/comir/). CoMir uses multiple microRNA databases (miRanda, PITA, TargetScan and miRSVR) to derive their prediction score, which reflects the probability that a gene is targeted by a microRNA or set of microRNAs (Coronnello and Benos, 2013). We identified the combined predicted targets of miRNAs-142-3p, 142-5p, 223-3p, 32-5p and 200b-3p. For each gene we summed the probability score of the five individual microRNAs and selected genes having a total score ≥ 3 (maximum of 5) for anti-correlation analysis.

As the second stage in our microRNA target identification strategy, we used gene expression profiles of a subset of samples. From genome-wide microarray gene expression data we focused on genes meeting two primary criteria: 1) predicted as targets from our computational analysis; and 2) having a gene expression profile with a significant negative correlation to the microRNA qPCR data. Anti-correlated genes have been successfully used to identify microRNA targets in a range of studies (Wang and Li, 2009; Stempor et al., 2012; Gennarino et al., 2009).

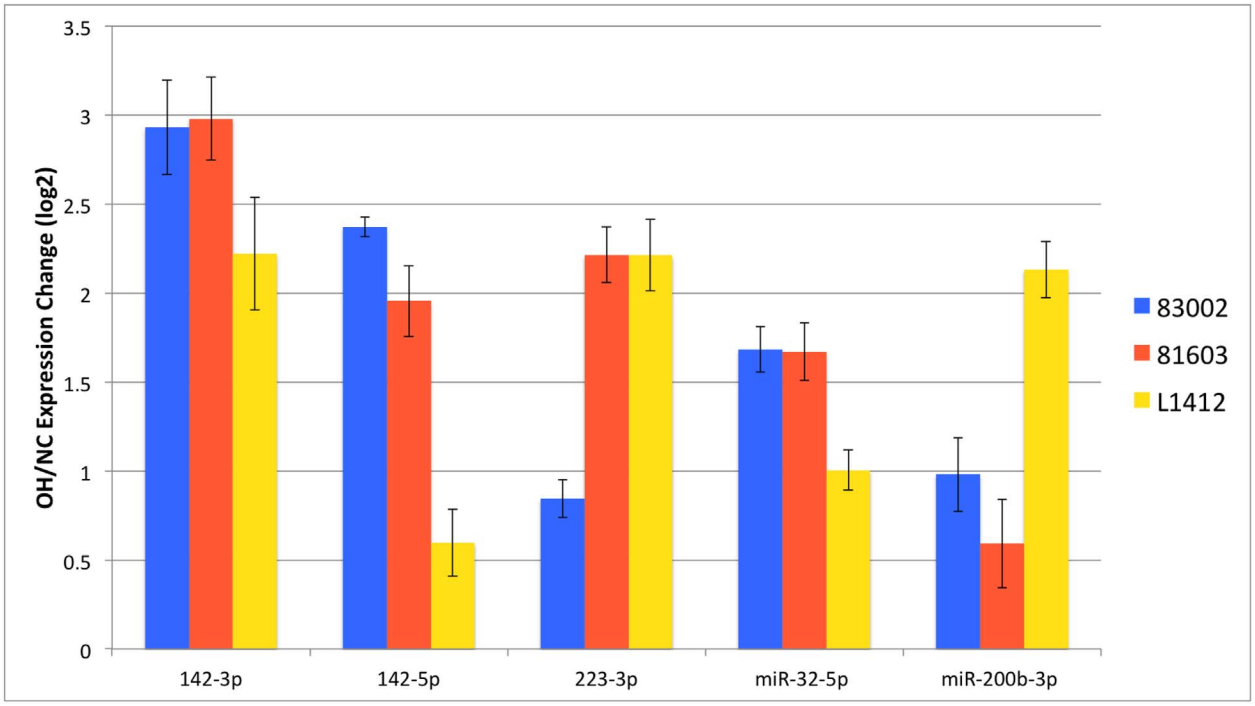

Fig. 2. The trend of microRNA induction is consistent in patient-matched pairs of tissues. OH/NC fold changes were calculated for patient-matched pairs of OH and NC tissues from three subjects (83002, 81603, L1412RK). Fold change values (log2) were derived from qPCR expression data. Error bars represent standard error of the mean.

To accomplish the anti-correlation analysis we used a subset of six samples that included each of the major categories: onset/AMT-hot, non-onset/AMT-cold, and onset/AMT-cold. The samples were selected to cover a representative range of miRNA levels, as well as provide matched pairs of samples where possible. We then performed gene expression microarray analysis on the samples. For predicted target genes identified in our CoMir computational analysis (above) we used the gene expression array data to perform anti-correlation analysis against the miRNA expression data from qPCR (miR-142-3p, 142-5p, 223-3p, 200b-3p and 32-5p). We calculated the correlation

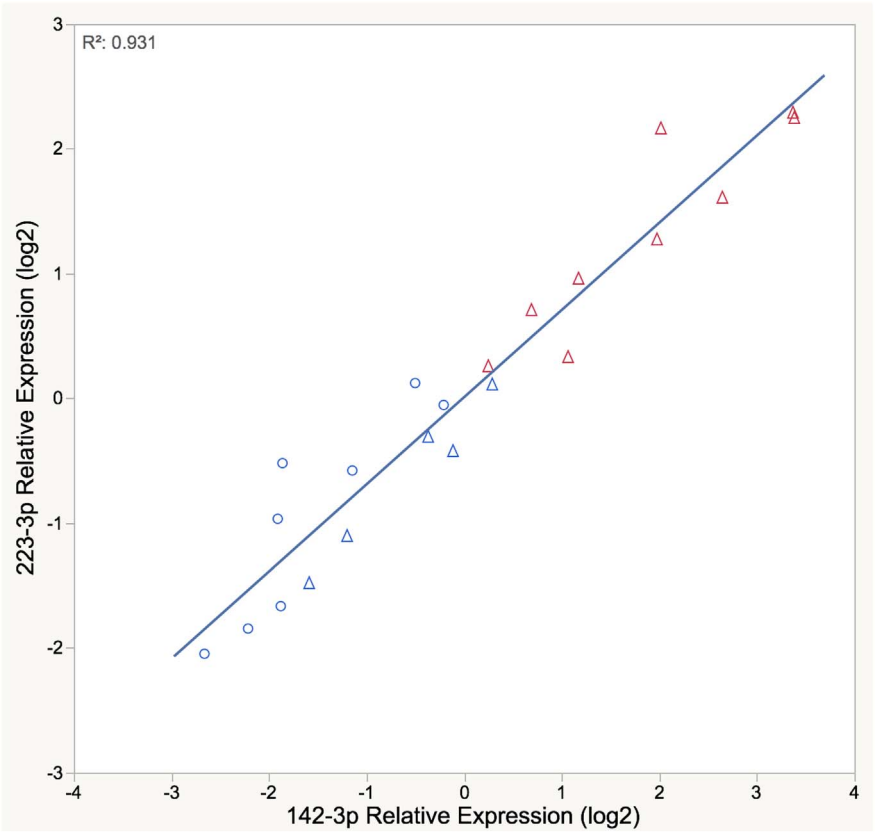

Fig. 3. Seizure onset/AMT-hot tubers have elevated levels of miRs 142-3p and 223-3p. Expression levels measured with qPCR reveal coincident induction of miRs-142-3p and -223-3p in seizure onset/AMT-hot TSC tubers (R^2 = 0.931). All onset/AMT-hot tubers had elevated expression of the two microRNAs.

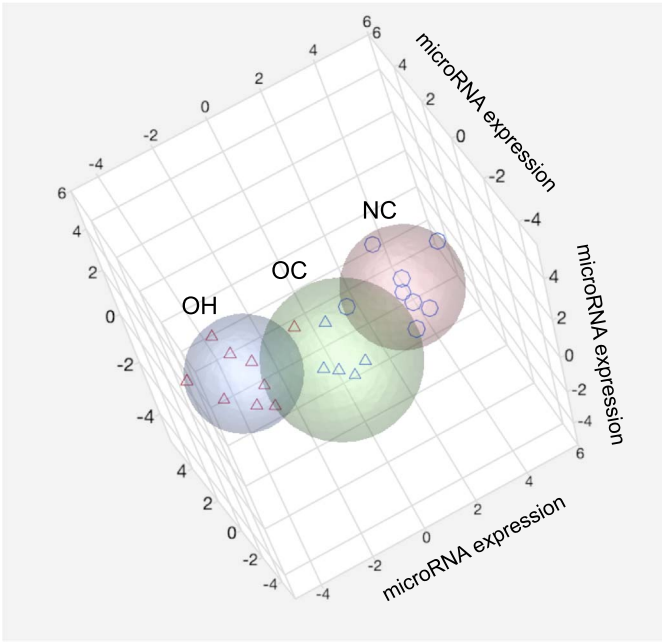

Fig. 4. Linear discriminant analysis (LDA) demonstrates that expression profiles of the five microRNAs can distinguish cortical tubers by their seizure onset propensity and AMT-PET uptake status. The axes represent linear combinations of the microRNA expression values, optimally selected to discriminate the tuber categories. Each sample is represented by the respective tuber category symbol (onset/AMT-hot (OH): red triangles; onset/AMT-cold (OC): blue triangles; non-onset/AMT-cold (NC): blue circles). Colored ellipses represent the 95% confidence region for each category. The correct tuber category is predicted for 95% of samples.

coefficient and associated P-value, comparing the gene expression data to the microRNA qPCR expression data. From the results we selected 395 genes with a significant anti-correlation ($P \leq 0.05$) between the microRNAs and target gene expression (Supplementary Table 2).

We submitted the list of 395 anti-correlated target genes to DAVID for functional analysis. DAVID (Database for Annotation, Visualization and Integrated Discovery) is an online tool that integrates a wide range of databases (e.g. gene ontology, pathway, etc.) for functional annotation analysis of large set of genes (Huang da et al., 2009a; Huang da et al., 2009b). We applied DAVID to identify functional categories enriched in our set of 395 target genes. Using functional categories based on UniProt keywords, the top categories having statistical significance and enriched at least 2-fold among our 395 target genes were synapse (20 genes), ion-transport (30 genes), and epilepsy (13 genes). The P-values and fold enrichment for each category are shown in Table 3 and the genes are provided in Table 4. We focused on the genes in the synapse, ion-transport, and epilepsy categories for additional investigation and found considerable overlap between the three groups. In addition to the evidence showing repression of these gene targets from our microarray expression data, we queried the data from our previous proteomics analysis that compared seizure onset tubers to non-tuber control tissue (Dombkowski et al., 2016). For those genes where the corresponding protein was available in the proteomics data, we found that 92% (12/13) of the synapse genes and 78% (7/9) of the epilepsy genes were also downregulated at the protein level in onset tubers in comparison to non-tuber control tissue. A scatter plot highlighting the consistent decrease of the proteins in these ontologies is shown in Supplementary Fig. 1, and the fold changes for each protein are provided in Supplementary Table 3.

We selected a subset of target genes from the three functional categories for additional validation. We performed qPCR analysis of *SYT1*, *GRIN2A*, *GRIN2B*, *KCNB1*, *SLC12A5*, *SCN2A*, *TSC1*, and *MEF2C*, measuring gene expression in each of our tuber specimens. As expected, each gene had a statistically significant negative correlation with the targeting microRNA having the highest prediction score (Table 5).

Table 3
Predicted target genes are enriched for functional processes associated with synapse, ion transport, and epilepsy risk. Functional annotation analysis (DAVID) was performed on 395 predicted target genes having significant anti-correlation to DE microRNAs (miRs-142-3p, -142-5p, 223-3p, 200b-3p and 32-5p). Fold-enrichment reflects the fraction of target genes in the annotated category as compared to what is expected by chance, given genome-wide abundance of genes in the given category.

Category	Number of genes	P-value	Fold-enrichment
Epilepsy	13	7.30E-07	6.5
Synapse	20	3.80E-06	3.6
Ion-transport	30	3.30E-07	3.0

3.5. Luciferase reporter assay confirms the interaction of miR-32-5p and SLC12A5

Our computational analysis and target gene expression profiling revealed that *SLC12A5 (KCC2*, solute carrier family 12 member 5) is a high confidence target of miR-32-5p. The highest scoring microRNA found in target predictions for *SLC12A5* is miR-32-5p. Our qPCR analysis confirmed a highly significant anti-correlation between *SLC12A5* expression and miR-32-5p in the tuber samples ($R^2 = 0.619$, $P < 0.0001$, Fig. 5A), and *SLC12A5* expression was significantly lower in OH tubers compared to either OC or NC tubers ($P = 0.0294$ and 0.0291 respectively). *SLC12A5* has recently been implicated in epilepsy (Kahle et al., 2016). To test the direct interaction between miR-32-5p and the *SLC12A5* 3′ UTR we performed a luciferase reporter assay to overexpress miR-32-5p in the presence of a reporter gene which contained the *SLC12A5* 3′ UTR. We found that miR-32-5p expression caused a 67% decrease of the reporter, compared to a scrambled miRNA control (Fig. 5B). Our results confirm that miR-32-5p interacts with the *SLC12A5* 3′ UTR and represses the transcript.

4. Discussion

We previously reported aberrant microRNA activity in tubers from TSC patients undergoing epilepsy surgery by comparing expression profiles in seizure onset tubers to adjacent non-tuber tissue (Dombkowski et al., 2016). The observed expression differences in that study represented the combined effect of the lesion and its epileptogenic potential. In the current study we sought to identify microRNA activity that is specific to epileptogenic potential and whether there was increased tryptophan metabolism measured in vivo with PET, with the hypothesis that microRNA activity may contribute to the epileptogenesis of tubers and inflammatory processes related to increased tryptophan metabolism in seizure onset tubers. By directly comparing seizure onset tubers, with and without increased AMT uptake, and non-onset tubers we have avoided confounding effects that may arise due to differences in cell type composition if comparing only tuber to non-tuber control tissue. Our TSC tissue archive included a number of matched pairs where both types of tissue were available from the same patient, providing additional within-subject control.

Using microarrays followed by qPCR validation, we identified five microRNAs (miRs-142-3p, 142-5p, 223-3p, 200b-3p and 32-5p) that were significantly elevated in seizure onset/AMT-hot tubers compared to non-onset/AMT-cold tubers and onset/AMT-cold tubers. Statistical analysis of qPCR results showed that induction of the microRNAs was most significantly associated with AMT-PET uptake. Linear discriminant analysis demonstrated that the aggregate expression pattern for the five microRNAs was distinct among the three tuber categories and could correctly predict the combined onset and AMT status for 95% of samples. This finding suggests a functional role for the microRNAs in TSC tuber epileptogenesis and that the magnitude of this effect is

Table 4
Target genes in the enriched functional categories of synapse (S), ion transport (I), and epilepsy (E). Each gene was predicted as a high confidence target by computational analysis and also had a significant anti-correlation of expression compared to the targeting microRNA.

UNIGENE	Gene symbol	Description	Category
Hs.483239	ALDH7A1	Aldehyde dehydrogenase 7 family, member A1	E
Hs.4993	PCDH19	Protocadherin 19	E
Hs.649965*	**MEF2C**	**Myocyte enhancer factor 2C**	**E**
Hs.655684	CNTNAP2	Contactin associated protein-like 2	E
Hs.370854	TSC1	Tuberous sclerosis 1	E
Hs.553187	KCNH1	Potassium channel, voltage gated eag related subfamily H, member 1	E, I
Hs.21413*	**SLC12A5**	**Solute carrier family 12 member 5**	**E, I**
Hs.436550*	SCN8A	Sodium voltage-gated channel alpha subunit 8	E, I
Hs.506759	ATP2A2	ATPase sarcoplasmic/endoplasmic reticulum Ca2 + transporting 2	E, I
Hs.93485*	**SCN2A**	**Sodium voltage-gated channel alpha subunit 2**	**E, I**
Hs.411472*	**GRIN2A**	**Glutamate ionotropic receptor NMDA type subunit 2A**	**E, I, S**
Hs.654430*	**GRIN2B**	**Glutamate ionotropic receptor NMDA type subunit 2B**	**E, I, S**
Hs.84244*	**KCNB1**	**Potassium voltage-gated channel subfamily B member 1**	**E, I, S**
Hs.118262	CACNA1C	Calcium channel, voltage-dependent, L type, alpha 1C subunit	I
Hs.658489	CLCC1	Chloride channel CLIC-like 1	I
Hs.134190	NIPAL1	NIPA-like domain containing 1	I
Hs.148907	SLC5A12	Solute carrier family 5 member 12	I
Hs.153521	KCNC4	Potassium voltage-gated channel subfamily C member 4	I
Hs.250083	SLC9A2	Solute carrier family 9 member A2	I
Hs.274579	CNNM1	Cyclin and CBS domain divalent metal cation transport mediator 1	I
Hs.47288	TRPM3	Transient receptor potential cation channel subfamily M member 3	I
Hs.506276	ATP2B1	ATPase plasma membrane Ca2 + transporting 1	I
Hs.514870	ATP5F1	ATP synthase, H + transporting, mitochondrial Fo complex subunit B1	I
Hs.411299	KCNJ15	Potassium channel, inwardly rectifying subfamily J, member 15	I
Hs.658533	KCNJ6	Potassium voltage-gated channel subfamily J member 6	I
Hs.482017	LRRC8B	Leucine rich repeat containing 8 family, member B	I
Hs.5462	SLC4A4	Solute carrier family 4 member 4	I
Hs.4749	SLC4A8	Solute carrier family 4, sodium bicarbonate cotransporter, member 8	I
Hs.91389	SLC9A7	Solute carrier family 9 member A7	I
Hs.516866	SLC23A2	Solute carrier family 23 (ascorbic acid transporter), member 2	I
Hs.385530	SLC24A4	Solute carrier family 24 (sodium/potassium/calcium exchanger), member 4	I
Hs.116250	GABRA2	Gamma-aminobutyric acid (GABA) A receptor, alpha 2	I, S
Hs.2700	GLRA2	Glycine receptor alpha 2	I, S
Hs.631595	CACNG8	Calcium voltage-gated channel auxiliary subunit gamma 8	I, S
Hs.661870	KCTD16	Potassium channel tetramerization domain containing 16	I, S
Hs.440379	ARHGAP32	Rho GTPase activating protein 32	S
Hs.370510	CADM1	Cell adhesion molecule 1	S
Hs.164578	CADM2	Cell adhesion molecule 2	S
Hs.535891	CHRM2	Cholinergic receptor, muscarinic 2	S
Hs.367656	DLG2	Discs large MAGUK scaffold protein 2	S
Hs.159291	DRP2	Dystrophin related protein 2	S
Hs.103183	FMR1	Fragile X mental retardation 1	S
Hs.478289	NLGN1	Neuroligin 1	S
Hs.655271	RIMS2	Regulating synaptic membrane exocytosis 2	S
Hs.21754	SV2B	Synaptic vesicle glycoprotein 2B	S
Hs.310545*	**SYT1**	**Synaptotagmin 1**	**S**
Hs.32984	SYT11	Synaptotagmin 11	S
Hs.569438	TLN2	Talin 2	S

*Bold text: validated with qPCR.
I: ion transport.
S: synapse.
E: epilepsy.

Table 5
Validation of target gene expression. Predicted target genes were significantly anti-correlated in expression, compared to the microRNA having the highest prediction score. Expression values were measured for the target gene and microRNA in each tuber using qPCR.

Target gene	microRNA	R^2	P
GRIN2A	200b-3p	0.627	< 0.0001
GRIN2B	142-5p	0.725	< 0.0001
KCNB1	200b-3p	0.602	< 0.0001
MEF2C	223-3p	0.476	0.0004
SCN2A	142-5p	0.583	< 0.0001
SLC12A5	32-5p	0.619	< 0.0001
SYT1	142-5p	0.789	< 0.0001
TSC1	200b-3p	0.427	0.001

greatest in seizure onset tubers with increased tryptophan metabolism measured by AMT PET.

The potential role of the five microRNAs in the epileptogenesis of TSC tubers is supported by other reports implicating these miRs in epilepsy. Both miR-142-3p and 5p were upregulated in pilocarpine induced status epilepticus (SE) in rats (Risbud and Porter, 2013). Kretschmann et al. reported upregulation of miR-142-5p in two different models of chronic epilepsy and a 6 Hz seizure-model in mouse (Kretschmann et al., 2015). They also found miR-223-3p upregulated in a pilocarpine mouse model of chronic epilepsy. Gorter et al. found upregulation of miR-142-5p and miR-223 in the hippocampus of SE rats (Gorter et al., 2014). miR-32-5p was also found to be upregulated in kainic acid induced SE in mouse, along with miR-142-3p (Schouten et al., 2015).

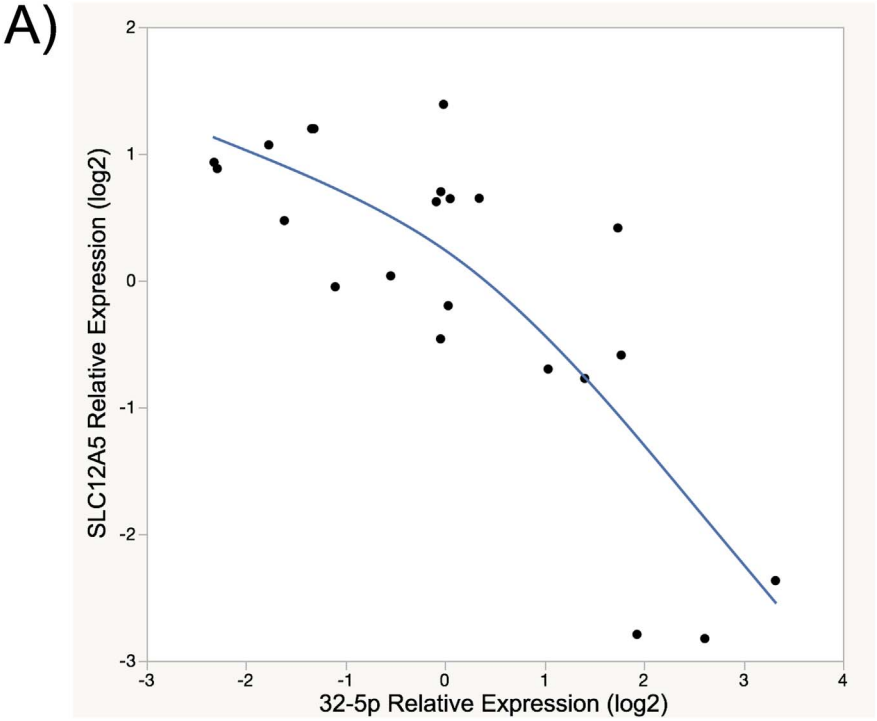

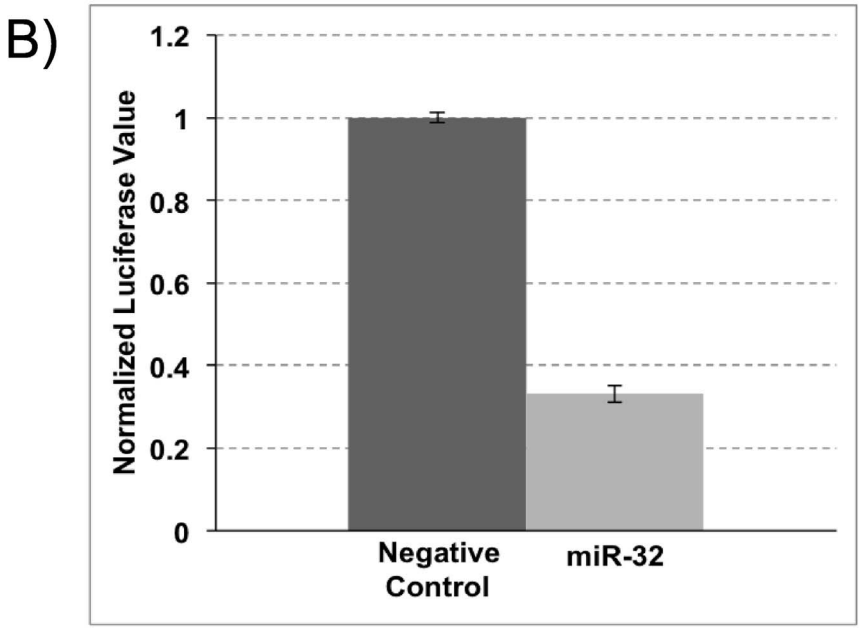

Fig. 5. miR-32-5p targets and inhibits SLC12A5 at the transcript level. Computational analysis revealed that the highest scoring microRNA predicted to target the SLC12A5 3′ UTR was miR-32-5p. A) Gene and microRNA expression profiles measured with qPCR demonstrate a significant anti-correlation between miR-32-5p and SLC12A5 expression in our set of TSC tubers ($P \leq 0.0001$). B) A luciferase reporter assay was used to confirm that miR-32 directly targets the 3′ UTR of SLC12A5 and causes transcript repression.

Interestingly, Terlinska et al. recently compared serum miRNA profiles in TSC patients to non-TSC controls and found miR-142-3p and miR-142-5p levels to be *lower* in TSC patients (Trelinska et al., 2016). After 3 months of treatment with the mTOR inhibitor everolimus miR-142-3p levels rose above baseline, suggesting that mTOR activity is associated with a decrease in miR-142. Their results may appear inconsistent with the elevation of these microRNAs that we observed in TSC onset tuber tissue. However, the disparate behavior of miR-142 levels in plasma and brain tissue was also reported in a rat model of epilepsy (Roncon et al., 2015). The investigators found that miR-142-3p was upregulated after SE (during latency) in the granule cell layer of the hippocampus in a pilocarpine model. However, the same microRNA was down-regulated in plasma of the rats during the chronic stage. Similarly, the study of Gorter et al. found elevated levels of miR-142-5p in three brain regions during the latency period of a rat model of SE, and while they found increased levels of the microRNA in plasma at 24 h post-SE, it was not increased in plasma in the latent and chronic stages (Gorter et al., 2014). The Terlinska study did not measure tissue levels of the microRNAs, and the source of circulating miR-142 is currently unknown. The systemic manifestations of TSC could also affect circulating levels of microRNAs. Nonetheless, the results of Terlinska et al. and the animal models demonstrate that miR-142 can circulate at appreciable levels in serum or plasma and can be altered due to pathogenic processes and treatment (Trelinska et al., 2016; Makino et al., 2012; Kaduthanam et al., 2013). Subsequent investigations to further characterize miR-142, as well as the other microRNAs, in epileptic

brain tissue and determine their relationship to circulating levels may enable future use of the microRNAs in clinical applications.

To further understand the functional impact of the dysregulated microRNAs in tubers we utilized a two-stage approach to identify a set of 395 high confidence target genes. Functional annotation analysis of this set of genes revealed that the most enriched functional categories were synapse, ion transport, and epilepsy. We used qPCR to confirm expression profiles for several of the genes: *SLC12A5*, *SYT1*, *GRIN2A*, *GRIN2B*, *KCNB1*, *SCN2A*, *MEF2C and TSC1*. Each of these genes was confirmed to have a statistically significant anti-correlation with the targeting microRNA in the tuber samples, and all have been implicated in a variety of neurological disorders, including epilepsy. *MEF2C* and *GRIN2B* were previously demonstrated to be targets of miR-223-3p (Rangrez et al., 2012; Harraz et al., 2012), which further validates our approach to identification of targets of the microRNAs. Additionally, *TSC1* was previously shown to be a target of miR-32-5p (Suh et al., 2012). In our computational predictions miR-200b-3p had the highest score for *TSC1* out of the five microRNAs. It was closely followed by miR-32-5p, and qPCR validation demonstrated anti-correlated expression between *TSC1* and these two microRNAs.

We used a luciferase reporter assay to confirm the interaction of miR-32-5p and the *SLC12A5* 3′ UTR, resulting in transcriptional repression. Dysregulation of *SLC12A5* has been implicated in several neurological disorders such as schizophrenia and Huntington's (Kahle et al., 2016; Tao et al., 2012; Kalathur et al., 2015). Importantly, *SLC12A5* has recently become a focus for its potential role in human epilepsy (Kahle et al., 2016). *SLC12A5* is exclusively expressed in neurons where it functions as the principal K-Cl cotransporter (Gamba, 2005; Blaesse et al., 2009). Increased expression of *SLC12A5* during postnatal development mediates the switch of GABA from excitatory to inhibitory (Rivera et al., 1999; Cherubini et al., 1991; Ben-Ari et al., 1989). Inhibition of *SLC12A5* transcript by miR-92, a microRNA similar in sequence to miR-32-5p, has previously been reported (Barbato et al., 2010). Loss of function mutations in *SLC12A5* have been reported in patients with a type of infantile-onset pharmacoresistant epilepsy (Stodberg et al., 2015). Previous reports have noted the repression of *SLC12A5* in TSC tubers (Talos et al., 2012; Shimizu-Okabe et al., 2011; Ruffolo et al., 2016). Our finding of microRNA mediated repression of *SLC12A5* in onset/AMT-hot tubers warrants subsequent mechanistic studies to characterize its role in TSC epileptogenesis.

We found an exceptional correlation between miRs 142-3p and 223-3p in tubers, and elevated expression of these two microRNAs was found in all seizure onset/AMT-hot tubers. It is unclear if these microRNAs are directly involved in driving the uptake of AMT in the tubers, via kynurenine pathway activation, or if they are induced by the same signaling cascade that activates this pathway in onset tubers. Collectively, our results and the literature provide support for the latter hypothesis. Indoleamine 2,3-dioxygenase (*IDO1*) is the key rate-limiting enzyme in the kynurenine pathway, and elevated *IDO1* expression is correlated with AMT uptake in epileptogenic tubers (Chugani, 2011). *IDO1* is known to be activated by *IFN*γ, yet *IFN*γ is decreased in *TSC1* and *TSC2* null cell lines and tumors (El-Hashemite and Kwiatkowski, 2005). Recent reports show that *NF-kB* can also stimulate *IDO1* activity (Tas et al., 2007). The strong association that we have found between miRs-142-3p, 223-3p, and AMT PET in onset tubers may reflect that the microRNA induction and AMT uptake are concerted responses to the same inflammatory signaling mediated through *NF-kB*. *NF-kB* is a key signaling component of the inflammatory response, and elevated *NF-kB* signaling has been reported in TSC tubers (Dombkowski et al., 2016; Maldonado et al., 2003). A recent report has shown that *NF-kB* and Notch are co-regulatory transcriptional activators of miR-223 through transcription factor binding sites in the microRNA promoter region (Kumar et al., 2014). Interestingly, the data from that study shows that both miR-223 and 142-3p were repressed in response to *NOTCH3* knockdown in Jurkat cells. Furthermore, recent reports have shown elevated Notch signaling as a result of inactivating TSC mutations, mediated through *Rheb* (Pear, 2010; Ma et al., 2010; Karbowniczek et al., 2010). Together, NOTCH and *NF-kB* activation in TSC are potential inducers of miRs-142-3p and 223-3p.

We have identified a microRNA expression signature that clearly distinguishes TSC tubers by their seizure onset propensity and elevated tryptophan metabolism, measured by AMT PET. The microRNA expression pattern appears to represent a progression from non-onset/AMT-cold tubers to onset/AMT-hot tubers, with onset/AMT-cold tubers an intermediate type. The inflammatory signaling events that are believed to drive the development of seizures in TSC (Boer et al., 2008; Zhang et al., 2015; He et al., 2013; Aronica and Crino, 2011) may be causing induction of these microRNAs, which subsequently repress known epilepsy risk genes and many genes involved in synaptic signaling. We will explore this mechanistic model in subsequent studies. A limitation of our study is the paucity of *TSC1* samples. Our rigorous sample selection required unambiguous MRI, ECoG, and AMT PET categorization for each sample and therefore excluded a number of potential specimens in our biorepository. Since *TSC1* patients comprise only ~15% of the TSC population and their phenotype is generally less severe than *TSC2* (Dabora et al., 2001; Au et al., 2007), the available *TSC1* tissue meeting the above requirements was very limited. It is unclear if the microRNA profiles found in our study will be similarly observed across a cohort of *TSC1* patients, and this warrants subsequent investigation as suitable *TSC1* samples become available. Our hypothesis of concerted Notch and *NF-kB* signaling as inducers of miRs 142-3p and 223-3p, downstream of TSC gene inactivation and the inflammatory response, leads to the expectation that these microRNAs would be overexpressed in *TSC1* onset tubers as well. Nonetheless, our findings are pertinent to the considerably larger fraction of *TSC2* patients, and they offer new insight as to why some tubers are epileptogenic while others are not.

Supplementary data to this article can be found online at https://doi.org/10.1016/j.nbd.2017.10.004.

Funding

This work was supported by the U.S. National Institutes of Health (1R01NS079429 [A.D.], 5R01NS064989 [H.C.], R01NS045151 [D.C.]), the U.S. Department of Defense CDMRP TSC research program (TS130067 [A.D.]), and the Children's Hospital of Michigan Foundation (R2-2016-46 [A.D.] and R1-2014-69 [A.D.]).

Acknowledgements

We would like to thank the TSC families that made this study possible. We would also like to thank Dr. Ajay Kumar for assistance with analysis of AMT PET results and Dr. Andrew Fribley for assistance with the luciferase assay.

References

Aronica, E., Crino, P.B., 2011. Inflammation in epilepsy: clinical observations. Epilepsia 52 (Suppl. 3), 26–32.

Aronica, E., Fluiter, K., Iyer, A., Zurolo, E., Vreijling, J., van Vliet, E.A., Baayen, J.C., Gorter, J.A., 2010. Expression pattern of miR-146a, an inflammation-associated microRNA, in experimental and human temporal lobe epilepsy. Eur. J. Neurosci. 31, 1100–1107.

Arya, R., Tenney, J.R., Horn, P.S., Greiner, H.M., Holland, K.D., Leach, J.L., Gelfand, M.J., Rozhkov, L., Fujiwara, H., Rose, D.F., Franz, D.N., Mangano, F.T., 2015. Long-term outcomes of resective epilepsy surgery after invasive presurgical evaluation in children with tuberous sclerosis complex and bilateral multiple lesions. J. Neurosurg. Pediatr. 15, 26–33.

Asano, E., Chugani, D.C., Muzik, O., Shen, C., Juhasz, C., Janisse, J., Ager, J., Canady, A., Shah, J.R., Shah, A.K., Watson, C., Chugani, H.T., 2000. Multimodality imaging for improved detection of epileptogenic foci in tuberous sclerosis complex. Neurology 54, 1976–1984.

Asano, E., Juhasz, C., Shah, A., Sood, S., Chugani, H.T., 2009. Role of subdural electrocorticography in prediction of long-term seizure outcome in epilepsy surgery. Brain 132, 1038–1047.

Au, K.S., Williams, A.T., Roach, E.S., Batchelor, L., Sparagana, S.P., Delgado, M.R.,

Wheless, J.W., Baumgartner, J.E., Roa, B.B., Wilson, C.M., Smith-Knuppel, T.K., Cheung, M.Y., Whittemore, V.H., King, T.M., Northrup, H., 2007. Genotype/phenotype correlation in 325 individuals referred for a diagnosis of tuberous sclerosis complex in the United States. Genet. Med. 9, 88–100.
Barbato, C., Ruberti, F., Pieri, M., Vilardo, E., Costanzo, M., Ciotti, M.T., Zona, C., Cogoni, C., 2010. MicroRNA-92 modulates K(+) Cl(−) co-transporter KCC2 expression in cerebellar granule neurons. J. Neurochem. 113, 591–600.
Ben-Ari, Y., Cherubini, E., Corradetti, R., Gaiarsa, J.L., 1989. Giant synaptic potentials in immature rat CA3 hippocampal neurones. J. Physiol. 416, 303–325.
Blaesse, P., Airaksinen, M.S., Rivera, C., Kaila, K., 2009. Cation-chloride cotransporters and neuronal function. Neuron 61, 820–838.
Boer, K., Spliet, W.G., van Rijen, P.C., Redeker, S., Troost, D., Aronica, E., 2006. Evidence of activated microglia in focal cortical dysplasia. J. Neuroimmunol. 173, 188–195.
Boer, K., Jansen, F., Nellist, M., Redeker, S., van den Ouweland, A.M., Spliet, W.G., van Nieuwenhuizen, O., Troost, D., Crino, P.B., Aronica, E., 2008. Inflammatory processes in cortical tubers and subependymal giant cell tumors of tuberous sclerosis complex. Epilepsy Res. 78, 7–21.
Chaudhuri, A.D., Yelamanchili, S.V., Marcondes, M.C., Fox, H.S., 2013. Up-regulation of microRNA-142 in simian immunodeficiency virus encephalitis leads to repression of sirtuin1. FASEB J. 27, 3720–3729.
Cherubini, E., Gaiarsa, J.L., Ben-Ari, Y., 1991. GABA: an excitatory transmitter in early postnatal life. Trends Neurosci. 14, 515–519.
Chugani, D.C., 2011. Alpha-methyl-L-tryptophan: mechanisms for tracer localization of epileptogenic brain regions. Biomark. Med 5, 567–575.
Chu-Shore, C.J., Major, P., Camposano, S., Muzykewicz, D., Thiele, E.A., 2010. The natural history of epilepsy in tuberous sclerosis complex. Epilepsia 51, 1236–1241.
Coronnello, C., Benos, P.V., 2013. ComiR: combinatorial microRNA target prediction tool. Nucleic Acids Res. 41, W159–164.
Dabora, S.L., Jozwiak, S., Franz, D.N., Roberts, P.S., Nieto, A., Chung, J., Choy, Y.S., Reeve, M.P., Thiele, E., Egelhoff, J.C., Kasprzyk-Obara, J., Domanska-Pakiela, D., Kwiatkowski, D.J., 2001. Mutational analysis in a cohort of 224 tuberous sclerosis patients indicates increased severity of TSC2, compared with TSC1, disease in multiple organs. Am. J. Hum. Genet. 68, 64–80.
Dombkowski, A.A., Sultana, Z., Craig, D.B., Jamil, H., 2011. In silico analysis of combinatorial microRNA activity reveals target genes and pathways associated with breast cancer metastasis. Cancer Informat. 10, 13–29.
Dombkowski, A.A., Batista, C.E., Cukovic, D., Carruthers, N.J., Ranganathan, R., Shukla, U., Stemmer, P.M., Chugani, H.T., Chugani, D.C., 2016. Cortical tubers: windows into dysregulation of epilepsy risk and synaptic signaling genes by MicroRNAs. Cereb. Cortex 26, 1059–1071.
Ebert, M.S., Sharp, P.A., 2012. Roles for microRNAs in conferring robustness to biological processes. Cell 149, 515–524.
Edwards, H., Rubenstein, M., Dombkowski, A.A., Caldwell, J.T., Chu, R., Xavier, A.C., Thummel, R., Neely, M., Matherly, L.H., Ge, Y., Taub, J.W., 2016. Gene signature of high white blood cell count in B-precursor acute lymphoblastic leukemia. PLoS One 11, e0161539.
El-Hashemite, N., Kwiatkowski, D.J., 2005. Interferon-gamma-Jak-Stat signaling in pulmonary lymphangioleiomyomatosis and renal angiomyolipoma: a potential therapeutic target. Am. J. Respir. Cell Mol. Biol. 33, 227–230.
Fedi, M., Reutens, D.C., Andermann, F., Okazawa, H., Boling, W., White, C., Dubeau, F., Nakai, A., Gross, D.W., Andermann, E., Diksic, M., 2003. Alpha-[11C]-methyl-L-tryptophan PET identifies the epileptogenic tuber and correlates with interictal spike frequency. Epilepsy Res. 52, 203–213.
Gamba, G., 2005. Molecular physiology and pathophysiology of electroneutral cation-chloride cotransporters. Physiol. Rev. 85, 423–493.
Gennarino, V.A., Sardiello, M., Avellino, R., Meola, N., Maselli, V., Anand, S., Cutillo, L., Ballabio, A., Banfi, S., 2009. MicroRNA target prediction by expression analysis of host genes. Genome Res. 19, 481–490.
Gorter, J.A., Iyer, A., White, I., Colzi, A., van Vliet, E.A., Sisodiya, S., Aronica, E., 2014. Hippocampal subregion-specific microRNA expression during epileptogenesis in experimental temporal lobe epilepsy. Neurobiol. Dis. 62, 508–520.
Harraz, M.M., Eacker, S.M., Wang, X., Dawson, T.M., Dawson, V.L., 2012. MicroRNA-223 is neuroprotective by targeting glutamate receptors. Proc. Natl. Acad. Sci. U. S. A. 109, 18962–18967.
He, J.J., Wu, K.F., Li, S., Shu, H.F., Zhang, C.Q., Liu, S.Y., Yang, M.H., Yin, Q., Yang, H., 2013. Expression of the interleukin 17 in cortical tubers of the tuberous sclerosis complex. J. Neuroimmunol. 262, 85–91.
Huang da, W., Sherman, B.T., Lempicki, R.A., 2009a. Bioinformatics enrichment tools: paths toward the comprehensive functional analysis of large gene lists. Nucleic Acids Res. 37, 1–13.
Huang da, W., Sherman, B.T., Lempicki, R.A., 2009b. Systematic and integrative analysis of large gene lists using DAVID bioinformatics resources. Nat. Protoc. 4, 44–57.
Ibrahim, G.M., Morgan, B.R., Fallah, A., 2015. A partial least squares analysis of seizure outcomes following resective surgery for tuberous sclerosis complex in children with intractable epilepsy. Childs Nerv. Syst. 31, 181–184.
Jansen, F.E., van Huffelen, A.C., Algra, A., van Nieuwenhuizen, O., 2007. Epilepsy surgery in tuberous sclerosis: a systematic review. Epilepsia 48, 1477–1484.
Jimenez-Mateos, E.M., Bray, I., Sanz-Rodriguez, A., Engel, T., McKiernan, R.C., Mouri, G., Tanaka, K., Sano, T., Saugstad, J.A., Simon, R.P., Stallings, R.L., Henshall, D.C., 2011. miRNA expression profile after status epilepticus and hippocampal neuroprotection by targeting miR-132. Am. J. Pathol. 179, 2519–2532.
Juhasz, C., Buth, A., Chugani, D.C., Kupsky, W.J., Chugani, H.T., Shah, A.K., Mittal, S., 2013. Successful surgical treatment of an inflammatory lesion associated with new-onset refractory status epilepticus. Neurosurg. Focus. 34, E5.
Kaduthanam, S., Gade, S., Meister, M., Brase, J.C., Johannes, M., Dienemann, H., Warth, A., Schnabel, P.A., Herth, F.J., Sultmann, H., Muley, T., Kuner, R., 2013. Serum miR-142-3p is associated with early relapse in operable lung adenocarcinoma patients. Lung Cancer 80, 223–227.
Kagawa, K., Chugani, D.C., Asano, E., Juhasz, C., Muzik, O., Shah, A., Shah, J., Sood, S., Kupsky, W.J., Mangner, T.J., Chakraborty, P.K., Chugani, H.T., 2005. Epilepsy surgery outcome in children with tuberous sclerosis complex evaluated with alpha-[11C]methyl-L-tryptophan positron emission tomography (PET). J. Child Neurol. 20, 429–438.
Kahle, K.T., Khanna, A.R., Duan, J., Staley, K.J., Delpire, E., Poduri, A., 2016. The KCC2 cotransporter and human epilepsy: getting excited about inhibition. Neuroscientist 22, 555–562.
Kalathur, R.K., Giner-Lamia, J., Machado, S., Barata, T., Ayasolla, K.R., Futschik, M.E., 2015. The unfolded protein response and its potential role in Huntington's disease elucidated by a systems biology approach. In: F1000Res. 4. pp. 103.
Karbowniczek, M., Zitserman, D., Khabibullin, D., Hartman, T., Yu, J., Morrison, T., Nicolas, E., Squillace, R., Roegiers, F., Henske, E.P., 2010. The evolutionarily conserved TSC/Rheb pathway activates Notch in tuberous sclerosis complex and drosophila external sensory organ development. J. Clin. Invest. 120, 93–102.
Kosik, K.S., 2006. The neuronal microRNA system. Nat. Rev. Neurosci. 7, 911–920.
Kretschmann, A., Danis, B., Andonovic, L., Abnaof, K., van Rikxoort, M., Siegel, F., Mazzuferi, M., Godard, P., Hanon, E., Frohlich, H., Kaminski, R.M., Foerch, P., Pfeifer, A., 2015. Different microRNA profiles in chronic epilepsy versus acute seizure mouse models. J. Mol. Neurosci. 55, 466–479.
Kumar, A., Chugani, H.T., 2008. PET in the assessment of pediatric brain development and developmental disorders. PET Clin. 3, 487–515.
Kumar, A., Asano, E., Chugani, H.T., 2011. Alpha-[(1)(1)C]-methyl-L-tryptophan PET for tracer localization of epileptogenic brain regions: clinical studies. Biomark. Med 5, 577–584.
Kumar, V., Palermo, R., Talora, C., Campese, A.F., Checquolo, S., Bellavia, D., Tottone, L., Testa, G., Miele, E., Indraccolo, S., Amadori, A., Ferretti, E., Gulino, A., Vacca, A., Screpanti, I., 2014. Notch and NF-kB signaling pathways regulate miR-223/FBXW7 axis in T-cell acute lymphoblastic leukemia. Leukemia 28, 2324–2335.
Liu, D.Z., Tian, Y., Ander, B.P., Xu, H., Stamova, B.S., Zhan, X., Turner, R.J., Jickling, G., Sharp, F.R., 2010. Brain and blood microRNA expression profiling of ischemic stroke, intracerebral hemorrhage, and kainate seizures. J. Cereb. Blood Flow Metab. 30, 92–101.
Ma, J., Meng, Y., Kwiatkowski, D.J., Chen, X., Peng, H., Sun, Q., Zha, X., Wang, F., Wang, Y., Jing, Y., Zhang, S., Chen, R., Wang, L., Wu, E., Cai, G., Malinowska-Kolodziej, I., Liao, Q., Liu, Y., Zhao, Y., Sun, Q., Xu, K., Dai, J., Han, J., Wu, L., Zhao, R.C., Shen, H., Zhang, H., 2010. Mammalian target of rapamycin regulates murine and human cell differentiation through STAT3/p63/Jagged/Notch cascade. J. Clin. Invest. 120, 103–114.
Makino, K., Jinnin, M., Kajihara, I., Honda, N., Sakai, K., Masuguchi, S., Fukushima, S., Inoue, Y., Ihn, H., 2012. Circulating miR-142-3p levels in patients with systemic sclerosis. Clin. Exp. Dermatol. 37, 34–39.
Maldonado, M., Baybis, M., Newman, D., Kolson, D.L., Chen, W., McKhann 2nd, G., Gutmann, D.H., Crino, P.B., 2003. Expression of ICAM-1, TNF-alpha, NF kappa B, and MAP kinase in tubers of the tuberous sclerosis complex. Neurobiol. Dis. 14, 279–290.
Meza-Sosa, K.F., Valle-Garcia, D., Pedraza-Alva, G., Perez-Martinez, L., 2012. Role of microRNAs in central nervous system development and pathology. J. Neurosci. Res. 90, 1–12.
Nelson, P.T., Wang, W.X., Rajeev, B.W., 2008. MicroRNAs (miRNAs) in neurodegenerative diseases. Brain Pathol. 18, 130–138.
Pear, W.S., 2010. New roles for Notch in tuberous sclerosis. J. Clin. Invest. 120, 84–87.
Pereira, F., Mitchell, T., Botvinick, M., 2009. Machine learning classifiers and fMRI: a tutorial overview. NeuroImage 45, S199–209.
Rangrez, A.Y., M'Baya-Moutoula, E., Metzinger-Le Meuth, V., Henaut, L., Djelouat, M.S., Benchitrit, J., Massy, Z.A., Metzinger, L., 2012. Inorganic phosphate accelerates the migration of vascular smooth muscle cells: evidence for the involvement of miR-223. PLoS One 7, e47807.
Risbud, R.M., Porter, B.E., 2013. Changes in microRNA expression in the whole hippocampus and hippocampal synaptoneurosome fraction following pilocarpine induced status epilepticus. PLoS One 8, e53464.
Rivera, C., Voipio, J., Payne, J.A., Ruusuvuori, E., Lahtinen, H., Lamsa, K., Pirvola, U., Saarma, M., Kaila, K., 1999. The K+/Cl- co-transporter KCC2 renders GABA hyperpolarizing during neuronal maturation. Nature 397, 251–255.
Roncon, P., Soukupova, M., Binaschi, A., Falcicchia, C., Zucchini, S., Ferracin, M., Langley, S.R., Petretto, E., Johnson, M.R., Marucci, G., Michelucci, R., Rubboli, G., Simonato, M., 2015. MicroRNA profiles in hippocampal granule cells and plasma of rats with pilocarpine-induced epilepsy—comparison with human epileptic samples. Sci Rep 5, 14143.
Ruffolo, G., Iyer, A., Cifelli, P., Roseti, C., Muhlebner, A., van Scheppingen, J., Scholl, T., Hainfellner, J.A., Feucht, M., Krsek, P., Zamecnik, J., Jansen, F.E., Spliet, W.G., Limatola, C., Aronica, E., Palma, E., 2016. Functional aspects of early brain development are preserved in tuberous sclerosis complex (TSC) epileptogenic lesions. Neurobiol. Dis. 95, 93–101.
Schouten, M., Fratantoni, S.A., Hubens, C.J., Piersma, S.R., Pham, T.V., Bielefeld, P., Voskuyl, R.A., Lucassen, P.J., Jimenez, C.R., Fitzsimons, C.P., 2015. MicroRNA-124 and -137 cooperativity controls caspase-3 activity through BCL2L13 in hippocampal neural stem cells. Sci Rep 5, 12448.
Shimizu-Okabe, C., Tanaka, M., Matsuda, K., Mihara, T., Okabe, A., Sato, K., Inoue, Y., Fujiwara, T., Yagi, K., Fukuda, A., 2011. KCC2 was downregulated in small neurons localized in epileptogenic human focal cortical dysplasia. Epilepsy Res. 93, 177–184.
Stempor, P.A., Cauchi, M., Wilson, P., 2012. MMpred: functional miRNA–mRNA interaction analyses by miRNA expression prediction. BMC Genomics 13, 620.
Stodberg, T., McTague, A., Ruiz, A.J., Hirata, H., Zhen, J., Long, P., Farabella, I., Meyer, E., Kawahara, A., Vassallo, G., Stivaros, S.M., Bjursell, M.K., Stranneheim, H.,

Tigerschiold, S., Persson, B., Bangash, I., Das, K., Hughes, D., Lesko, N., Lundeberg, J., Scott, R.C., Poduri, A., Scheffer, I.E., Smith, H., Gissen, P., Schorge, S., Reith, M.E., Topf, M., Kullmann, D.M., Harvey, R.J., Wedell, A., Kurian, M.A., 2015. Mutations in SLC12A5 in epilepsy of infancy with migrating focal seizures. Nat. Commun. 6, 8038.

Suh, S.S., Yoo, J.Y., Nuovo, G.J., Jeon, Y.J., Kim, S., Lee, T.J., Kim, T., Bakacs, A., Alder, H., Kaur, B., Aqeilan, R.I., Pichiorri, F., Croce, C.M., 2012. MicroRNAs/TP53 feedback circuitry in glioblastoma multiforme. Proc. Natl. Acad. Sci. U. S. A. 109, 5316–5321.

Szafranski, K., Abraham, K.J., Mekhail, K., 2015. Non-coding RNA in neural function, disease, and aging. Front. Genet. 6, 87.

Talos, D.M., Sun, H., Kosaras, B., Joseph, A., Folkerth, R.D., Poduri, A., Madsen, J.R., Black, P.M., Jensen, F.E., 2012. Altered inhibition in tuberous sclerosis and type IIb cortical dysplasia. Ann. Neurol. 71, 539–551.

Tao, R., Li, C., Newburn, E.N., Ye, T., Lipska, B.K., Herman, M.M., Weinberger, D.R., Kleinman, J.E., Hyde, T.M., 2012. Transcript-specific associations of SLC12A5 (KCC2) in human prefrontal cortex with development, schizophrenia, and affective disorders. J. Neurosci. 32, 5216–5222.

Tas, S.W., Vervoordeldonk, M.J., Hajji, N., Schuitemaker, J.H., van der Sluijs, K.F., May, M.J., Ghosh, S., Kapsenberg, M.L., Tak, P.P., de Jong, E.C., 2007. Noncanonical NF-kappaB signaling in dendritic cells is required for indoleamine 2,3-dioxygenase (IDO) induction and immune regulation. Blood 110, 1540–1549.

Trelinska, J., Fendler, W., Dachowska, I., Kotulska, K., Jozwiak, S., Antosik, K., Gnys, P., Borowiec, M., Mlynarski, W., 2016. Abnormal serum microRNA profiles in tuberous sclerosis are normalized during treatment with everolimus: possible clinical implications. Orphanet. J. Rare Dis. 11, 129.

Wang, Y.P., Li, K.B., 2009. Correlation of expression profiles between microRNAs and mRNA targets using NCI-60 data. BMC Genomics 10, 218.

Wang, W.X., Visavadiya, N.P., Pandya, J.D., Nelson, P.T., Sullivan, P.G., Springer, J.E., 2015. Mitochondria-associated microRNAs in rat hippocampus following traumatic brain injury. Exp. Neurol. 265, 84–93.

Weiner, H.L., Carlson, C., Ridgway, E.B., Zaroff, C.M., Miles, D., LaJoie, J., Devinsky, O., 2006. Epilepsy surgery in young children with tuberous sclerosis: results of a novel approach. Pediatrics 117, 1494–1502.

Xu, S., Wei, J., Wang, F., Kong, L.Y., Ling, X.Y., Nduom, E., Gabrusiewicz, K., Doucette, T., Yang, Y., Yaghi, N.K., Fajt, V., Levine, J.M., Qiao, W., Li, X.G., Lang, F.F., Rao, G., Fuller, G.N., Calin, G.A., Heimberger, A.B., 2014. Effect of miR-142-3p on the M2 macrophage and therapeutic efficacy against murine glioblastoma. J. Natl. Cancer Inst. 106.

Zhang, B., Zou, J., Rensing, N.R., Yang, M., Wong, M., 2015. Inflammatory mechanisms contribute to the neurological manifestations of tuberous sclerosis complex. Neurobiol. Dis. 80, 70–79.

Zitron, I.M., Kamson, D.O., Kiousis, S., Juhasz, C., Mittal, S., 2013. In vivo metabolism of tryptophan in meningiomas is mediated by indoleamine 2,3-dioxygenase 1. Cancer Biol. Ther. 14, 333–339.